Dispersion analysis of FDTD schemes for doubly lossy media

Heh, Ding Yu; Tan, Eng Leong

2009

Heh, D. Y., & Tan, E. L. (2009). Dispersion analysis of FDTD schemes for doubly lossy media. Progress In Electromagnetics Research B, 17, 327-342. doi:10.2528/pierb09082802

https://hdl.handle.net/10356/137131

https://doi.org/10.2528/PIERB09082802

Progress In Electromagnetics Research B, Vol. 17, 327–342, 2009

DISPERSION ANALYSIS OF FDTD SCHEMES FOR DOUBLY LOSSY MEDIA

D. Y. Heh and E. L. Tan

School of Electrical and Electronic Engineering
Nanyang Technological University
50, Nanyang Avenue, Singapore 639798, Singapore

Abstract—This paper presents the 3-D dispersion analysis of finite-difference time-domain (FDTD) schemes for doubly lossy media, where both electric and magnetic conductivities are nonzero. Among the FDTD schemes presented are time-average (TA), time-forward (TF), time-backward (TB) and exponential time differencing (ETD). It is first shown that, unlike in electrically lossy media, the attenuation constant in doubly lossy media can be larger than its phase constant. This further calls for careful choice of cell size such that both wavelength and skin depth of the doubly lossy media are properly resolved. From the dispersion analysis, TF generally displays higher phase velocity and attenuation errors due to its first-order temporal accuracy nature compared to second-order ETD and TA. Although both have second-order temporal accuracy, ETD has generally lower phase velocity and attenuation errors than TA. This may be attributed to its closer resemblance to the solution of first-order differential equation. Numerical FDTD simulations in 1-D and 3-D further confirm these findings.

1. INTRODUCTION

The finite-diference time-domain (FDTD) method [1] has been successful thus far in solving various electromagnetics problems. In addition, the effects of lossy media and conductors have been treated by incorporating the conductivity into the original formulation of lossless FDTD update equations. By far, there are four known schemes for such purposes. One common scheme is the time-average (TA) [1]. Other variants include the time-forward (TF) [2], time-backward (TB) [3] and the exponential time differencing (ETD) [4, 5].

Corresponding author: E. L. Tan (eeltan@ntu.edu.sg).

Stability analysis in [6–8] showed that for an electrically lossy medium, TA still preserves the stability criterion as the lossless FDTD scheme, i.e., the Courant-Friedrichs-Lewy (CFL) limit. On the other hand, TF and ETD have more relaxed and TB, more stringent stability criterion compared to the lossless CFL limit. With such relaxed stabililty criterion for ETD and TF, [8] demonstrated that both ETD and TF allow for efficient simulation (with larger time step) of highly conductive media in 1-D compared to TA, while TB becomes practically unusable. The bottom line is that there is a trade-off between efficiency and accuracy if one were to choose between TA, ETD or TF. TA is chosen when the time step is driven at CFL limit (accuracy), while ETD or TF are used for time step beyond the CFL limit (efficiency). However, since ETD resembles closest to the solution of first-order differential equation (Maxwell's equations), it is of great interest to ascertain if ETD outperforms TA and other schemes at the same time step. Furthermore, the dispersion analysis of TA in [9] had been confined to only electrically lossy media, and it is often desirable to carry out the investigation for the more general doubly lossy media, where both electic and magnetic conductivities are nonzero. For instance, the media used for perfectly matched layer (PML) [10] as absorbing boundary conditions require nonzero electric and magnetic conductivities. Certain ferrite composites [11, 12], magnetic materials [13] and wave absorbers [14, 15] are also known to possess both electric and magnetic loss tangents, which find many applications in microwave engineering.

In this paper, we present the 3-D dispersion analysis of FDTD schemes for doubly lossy media, with more emphasis being placed on ETD, TA and TF. The lossless CFL limit will be applied for fair comparison, while time step used beyond the lossless CFL limit is beyond the scope of this paper. It will be shown that, if lossless CFL limit is applied for both ETD and TA, ETD generally exhibits lower dispersion errors compared to TA and hence should be favoured over TA. On the other hand, TF has higher dispersion errors compared to ETD and TA because it is only first-order accurate in time. Numerical simulations will further confirm these findings. It will also be shown that, unlike in electrically lossy media, the attenuation constant in doubly lossy media can be larger than its phase constant, which further calls for careful choice of cell size such that both wavelength and skin depth of the doubly lossy media are properly resolved.

2. FDTD SCHEMES FOR DOUBLY LOSSY MEDIA

Consider a source-free, isotropic, homogeneous doubly lossy medium. The Maxwell's curl equations in differential form are stated as

$$\epsilon\frac{\partial}{\partial t}\mathbf{E} - \sigma\mathbf{E} = \nabla \times \mathbf{H} \tag{1a}$$

$$\mu\frac{\partial}{\partial t}\mathbf{H} - \sigma^*\mathbf{H} = -\nabla \times \mathbf{E} \tag{1b}$$

where ϵ, σ, and μ, σ^* are the permittivity, electric conductivity and permeability, magnetic conductivity, respectively. Note that in practice, second-order central differencing is usually adopted for spatial derivatives (curl) in (1) and all fields are properly staggered on a Yee lattice. On the other hand, different ways of discretizing (1) in time will give rise to different schemes. In the following, we first provide a brief overview of some FDTD based schemes for electrically lossy media and extend for doubly lossy media. For discretization of Ampere's law (1a), we begin by expressing the exact solution to the first-order differential Equation (1a) as

$$\mathbf{E}(t) = e^{-\frac{(t-t_0)}{\tau}}\mathbf{E}(t_0) + \frac{1}{\epsilon}\int_{t_0}^{t} e^{-\frac{(t-t')}{\tau}}\left(\nabla \times \mathbf{H}\left(t'\right)\right)dt' \tag{2}$$

where t_0 is the initial time and $\tau = \epsilon/\sigma$. The generalized update equation of FDTD schemes for electric field can be written as

$$\mathbf{E}^{n+1} = c_{a,e}\mathbf{E}^n + c_{b,e}\nabla \times \mathbf{H}^{n+\frac{1}{2}} \tag{3}$$

where $c_{a,e}$ and $c_{b,e}$ are the electric field update coefficients.

The electric field update coefficients for ETD, TA, TF and TB are given as follows:

ETD: $c_{a,e}^{ETD} = e^{-\frac{\Delta t}{\tau}}$, $\quad c_{b,e}^{ETD} = \frac{1-e^{-\frac{\Delta t}{\tau}}}{\sigma}$

TA: $c_{a,e}^{TA} = \frac{1-\frac{\Delta t}{2\tau}}{1+\frac{\Delta t}{2\tau}}$, $\quad c_{b,e}^{TA} = \frac{\Delta t/\epsilon}{1+\frac{\Delta t}{2\tau}}$

TF: $c_{a,e}^{TF} = \frac{1}{1+\frac{\Delta t}{\tau}}$, $\quad c_{b,e}^{TF} = \frac{\Delta t/\epsilon}{1+\frac{\Delta t}{\tau}}$

TB: $c_{a,e}^{TB} = 1 - \frac{\Delta t}{\tau}$, $\quad c_{b,e}^{TB} = \frac{\Delta t}{\epsilon}$

We first note that the update coefficients of ETD are the closest compared to the analytical solution (1a). In fact, it should also be pointed out that by applying the following second-order Pade approximation to the ETD update coefficients,

$$e^{-t} = \frac{1-t/2}{1+t/2} + O(t^3) \tag{4}$$

we will recover the TA update coefficients. Therefore, TA is a further Pade approximation of the ETD scheme, though both schemes still maintain overall temporal accuracy of second-order. On the other hand, TF utilizes forward differencing for its time derivative and TB utilizes backward differencing, which result in only first-order accuracy in time.

For doubly lossy media, the discretization of Faraday's law (1b) follows in the similar manner. The generalized update equation for magnetic field is given as

$$\mathbf{H}^{n+1} = c_{a,h}\mathbf{H}^{n} - c_{b,h}\nabla \times \mathbf{E}^{n+\frac{1}{2}} \tag{5}$$

The magnetic field update coefficients $c_{a,h}$ and $c_{b,h}$ for all the schemes can then be obtained by replacing τ, ϵ, and σ in the previous electric field update coefficients with τ^*, μ, and σ^*, respectively, where $\tau^* = \mu/\sigma^*$.

3. DISPERSION ANALYSIS AND NUMERICAL SIMULATION FOR DOUBLY LOSSY MEDIA

By substituting the Fourier modes to all fields in the update equations detailed in the previous section, one will arrive at the generalized dispersion relation as follows:

$$\sum_{\xi=x,y,z} \left(\frac{2}{\Delta\xi}\sin(k_\xi \Delta\xi/2)\right)^2 \left(\frac{2}{\Delta t}\sin(\omega\Delta t/2)\right)^2 \mu_{nc}\epsilon_{nc} \tag{6}$$

where $\Delta\xi$ and k_ξ are spatial steps and wavenumbers in each x, y and z directions. ϵ_{nc} and μ_{nc} are known as the complex numerical permittivity and permeability which are unique to a particular FDTD scheme in doubly lossy media. Note that in lossless media, $\epsilon_{nc} = \epsilon$, $\mu_{nc} = \mu$ and (6) will recover the original dispersion relation of FDTD scheme in lossless media. The complex numerical permittivity of each scheme is shown clearly in Table 1. Also shown in Table 1 is the truncation error term in Δt compared to the analytical complex permittivity in doubly lossy media given by $\epsilon(\omega) = \epsilon - j\frac{\sigma}{\omega}$. On the other hand, complex numerical permeability of each scheme and their respective leading truncation error can be obtained simply by substituting σ, ϵ with σ^*, μ, respectively, and thus, shall not be repeated. For all discretization parameters Δx, Δy, Δz and Δt approaching zero, ϵ_{nc} approaches $\epsilon(\omega)$ and μ_{nc} approaches $\mu(\omega)$. From the table, TA and ETD have leading truncation error of second-order, while TF and TB show first-order leading truncation error. These further ascertain the temporal accuracy discussed in the previous section.

Table 1. Complex numerical permittivity and leading error term for FDTD schemes.

Scheme	Complex Numerical Permittivity	Leading Error Term
ETD	$\frac{\sigma\Delta t e^{j\omega\frac{\Delta t}{2}}\left(1-e^{-\Delta t\left(\frac{1}{\tau}+j\omega\right)}\right)}{j2\sin\left(\omega\frac{\Delta t}{2}\right)\left(1-e^{-\frac{\Delta t}{\tau}}\right)}$	$\Delta t^2\left(\frac{j\sigma\omega}{12}+\frac{\sigma^2}{12\epsilon}\right)$
TA	$\epsilon+\frac{\sigma\Delta t\cot\left(\omega\frac{\Delta t}{2}\right)}{2j}$	$\Delta t^2\left(\frac{j\sigma\omega}{12}\right)$
TF	$\epsilon+\frac{\sigma\Delta t}{2}+\frac{\sigma\Delta t\cot\left(\omega\frac{\Delta t}{2}\right)}{2j}$	$\Delta t\frac{\sigma}{2}$
TB	$\epsilon-\frac{\sigma\Delta t}{2}+\frac{\sigma\Delta t\cot\left(\omega\frac{\Delta t}{2}\right)}{2j}$	$-\Delta t\frac{\sigma}{2}$

3.1. Resolving Both Wavelength and Skin Depth

From Maxwell's equations, the analytical attenuation constant, α_0 and phase constant, β_0 in a doubly lossy medium can be solved as

$$\alpha_0=\omega\left\{\frac{\mu'\epsilon'}{2}\left[\sqrt{\left(1-\frac{\mu''\epsilon''}{\mu'\epsilon'}\right)^2+\left(\frac{\mu''}{\mu'}+\frac{\epsilon''}{\epsilon'}\right)^2}-\left(1-\frac{\mu''\epsilon''}{\mu'\epsilon'}\right)\right]\right\}^{\frac{1}{2}} \quad (7a)$$

$$\beta_0=\omega\left\{\frac{\mu'\epsilon'}{2}\left[\sqrt{\left(1-\frac{\mu''\epsilon''}{\mu'\epsilon'}\right)^2+\left(\frac{\mu''}{\mu'}+\frac{\epsilon''}{\epsilon'}\right)^2}+\left(1-\frac{\mu''\epsilon''}{\mu'\epsilon'}\right)\right]\right\}^{\frac{1}{2}} \quad (7b)$$

where $\epsilon'=\epsilon$, $\epsilon''=\sigma/\omega$, $\mu'=\mu$ and $\mu''=\sigma^*/\omega$. In electrically lossy media ($\sigma^*=0$), $\mu''=0$ and (7) will recover the propagation constant derived in most electromagnetic textbooks, e.g., [16]. The medium wavelength and skin depth can then be found by $2\pi/\beta_0$ and $1/\alpha_0$, respectively. In most previous numerical studies of electrically lossy media, the cell size of a particular FDTD scheme is selected such that it sufficiently resolves the wavelength of the medium (usually at least 1/10 of wavelength for tolerable numerical errors) while disregarding the skin depth. This is permissible in electrically lossy media due to the fact that α_0 is always smaller than β_0 if $\mu''=0$. In fact, in highly lossy conductor ($\epsilon''/\epsilon'\gg 1$), $\alpha_0\approx\beta_0$, and therefore, sufficiently resolved wavelength automatically guarantees sufficiently resolved skin depth. However in doubly lossy media, α_0 is not always smaller than β_0 for nonzero μ''. A closer look at (7) reveals that when $\mu''\epsilon''/\mu'\epsilon'>1$, $\alpha_0>\beta_0$. Under such circumstances, even if the wavelength is well resolved, the skin depth can be much smaller than the wavelength and still remains under-resolved which in turn yields higher numerical errors.

To further illustrate this, let us investigate the dispersion errors of FDTD schemes in doubly lossy media. We first assume 1-D propagation in z direction involving E_x and H_y field components. The only wavenumber k_z that exists can be solved explicitly from (6) as

$$k_z = \frac{2}{\Delta z} \arcsin\left(\frac{\Delta z\sqrt{\mu_{nc}\epsilon_{nc}}}{\Delta t} \sin\left(\frac{\omega \Delta t}{2}\right)\right) \tag{8}$$

The solution k_z will be complex in nature because of propagation in doubly lossy media. The numerical attenuation constant, phase constant and phase velocity can be found as $\alpha = -\Im(k_z)$, $\beta = \Re(k_z)$ and $v = \omega/\beta$ respectively. We further define two performance measures, which are the attenuation error, $(\alpha - \alpha_0)/\alpha_0$ and phase velocity error, $(v - v_0)/v_0$ where v_0 is the analytical phase velocity.

Figure 1 plots the phase velocity and attenuation errors with respect to $\sigma/\omega\epsilon$ with $\sigma^*/\omega\mu = 10^{-2}$ and cell per wavelength (CPW) equals 40. Δt is set at the 1-D lossless Courant limit $\Delta z\sqrt{\mu\epsilon}$ for ETD, TA, TF while for TB, smaller-than-lossless Courant limit is used due to the more stringent stability criterion. Note that the wavelength used is the wavelength in doubly lossy media, given by $2\pi/\beta_0$ and should not be confused with the lossless media wavelength $2\pi/(\omega\sqrt{\mu\epsilon})$. We first note that TF and TB generally have higher magnitudes of phase and attenuation errors compared to ETD and TA at lower $\sigma/\omega\epsilon$. This is expected as TF and TB are only first-order accurate in time while ETD and TA are both second-order. More importantly, regardless of schemes, we observe that both phase velocity and attenuation errors increase dramatically beyond $\sigma/\omega\epsilon = 10^2$ because it is beyond this point that $\alpha_0 > \beta_0$ and the skin depth becomes under-resolved. This indicates the necessity to properly resolve skin depth for $\mu''\epsilon''/\mu'\epsilon' > 1$, which will be shown later.

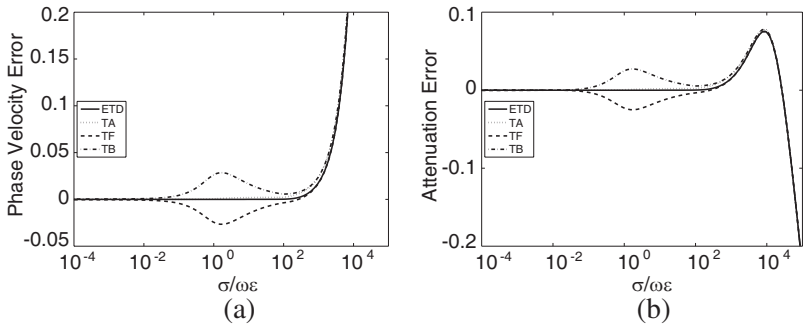

Figure 1. (a) Phase velocity and (b) attenuation errors with respect to $\sigma/\omega\epsilon$. $\sigma^*/\omega\mu = 10^{-2}$, CPW = 40.

3.2. 3-D Dispersion Analysis

Since the dispersion errors become increasingly large for $\mu''\epsilon''/\mu'\epsilon' > 1$, the skin depth will be properly resolved in the 3-D analysis here. In the subsequent analysis, instead of specifying only CPW, uniform cell size Δ is chosen such that for positive integer N, Δ is λ/N if $\mu''\epsilon''/\mu'\epsilon' \leq 1$, and $2\pi\delta_s/N$ if $\mu''\epsilon''/\mu'\epsilon' > 1$, where λ is the medium wavelength and δ_s is the skin depth. Larger N implies higher mesh density. These criteria will ensure that the cell size always properly resolves both wavelength and skin depth. 2π is included because the ratio between wavelength and skin depth is exactly 2π at $\alpha_0 = \beta_0$. Alternatively, one may also specify Δ in terms of the magnitude of complex wavenumber. The magnitude of complex wavenumber, $|k_0|$ can be found from (7) as

$$|k_0| = \sqrt{\alpha_0^2 + \beta_0^2} = \omega \left\{ \mu'\epsilon' \sqrt{\left(1 - \frac{\mu''\epsilon''}{\mu'\epsilon'}\right)^2 + \left(\frac{\mu''}{\mu'} + \frac{\epsilon''}{\epsilon'}\right)^2} \right\}^{\frac{1}{2}} \quad (9)$$

However, specifying Δ in this way may result in finer-than-necessary cell size, which increases computational effort undesirably, especially when $\alpha_0 = \beta_0$. Therefore, the former choice of specifying Δ in terms of λ or $2\pi\delta_s$ (depending on $\mu''\epsilon''/\mu'\epsilon'$) is preferred over the latter in terms of $|k_0|$. In 3-D, there exist three individual wave vectors, $k_x = k\sin\theta\cos\phi$, $k_y = k\sin\theta\sin\phi$ and $k_z = k\cos\phi$ where θ is the longitudinal angle, ϕ is the azimuthal angle and $k = \sqrt{k_x^2 + k_y^2 + k_z^2}$. The complex wavenumber k is then solved from (6) using appropriate root finding algorithm.

Figure 2 shows the 3-D plot of phase velocity error for all schemes at different propagation angle in the first octant. $\sigma/\omega\epsilon = \sigma^*/\omega\mu = 10^2$, which gives $\mu''\epsilon''/\mu'\epsilon' = 10^4 > 1$, and N is selected as 10. Δt is now set at the 3-D lossless Courant limit $\Delta\sqrt{3\mu\epsilon}$ for ETD, TA and TF while again for TB, it is set lower due to more stringent stability criterion. We see that, with properly resolved skin depth, the error level is not as high as in previous case. We also notice that second-order schemes ETD and TA have lower error magnitude than the first-order schemes TF and TB. On top of that, ETD has lower error compared to TA due to its closer resemblance to the solution of first-order differential equation. Furthermore, only TF has negative phase velocity error as opposed to others, which indicates that its phase velocity lags behind the analytical phase velocity while others lead. It will be shown later that for most of the values of $\sigma/\omega\epsilon$ and $\sigma^*/\omega\mu$, TF has opposing polarity of both phase velocity and attenuation errors compared to others. Since TB is only first-order accurate in time (higher error), and has more restrictive stability criterion compared to others, it shall

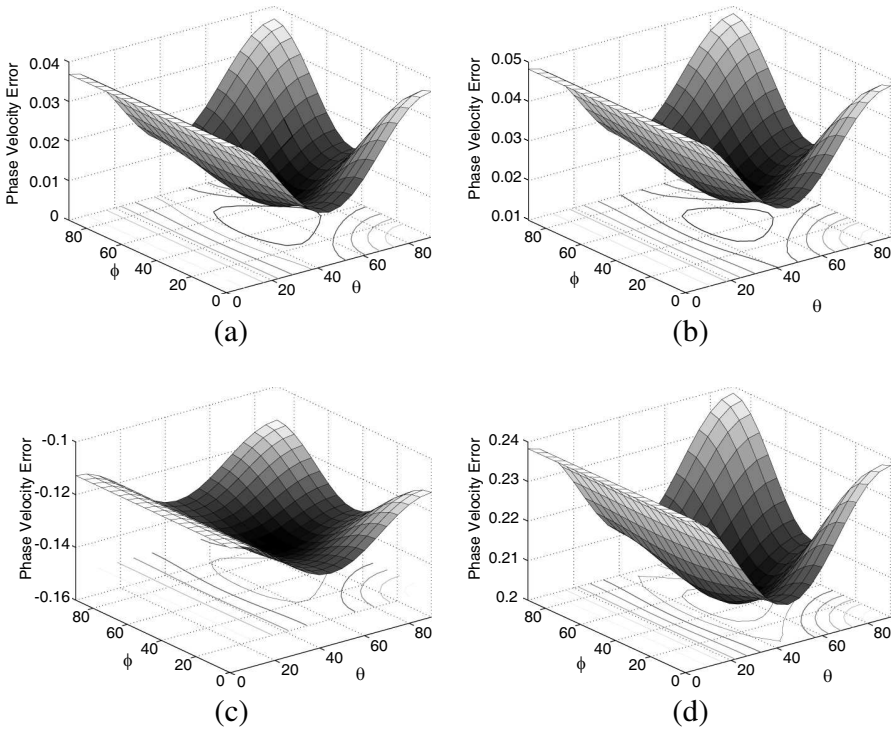

Figure 2. Phase velocity error for (a) ETD, (b) TA, (c) TF and (d) TB with respect to θ and ϕ. $\sigma/\omega\epsilon = \sigma^*/\omega\mu = 10^2$, $N = 10$.

be omitted in all our further comparisons. It should be reminded that unlike in 3-D lossless FDTD scheme where the numerical phase velocity always lags the analytical, it is generally not true in doubly lossy media. Also, the fact that lossless 3-D FDTD scheme always yields the lowest and highest phase velocity errors in the diagonal and axial directions does not generally apply for doubly lossy media.

In 3-D dispersion analysis, the more appropriate measures would be to find the maximum phase velocity and attenuation errors across all propagation angles (first octant will suffice as the dispersion error pattern repeats in every octant). We now define the positive maximum phase velocity error as $(\max[v(\theta,\phi)] - v_0)/v_0$ for $\max[v(\theta,\phi)] > v_0$, and the corresponding negative maximum phase velocity error as $(\min[v(\theta,\phi)] - v_0)/v_0$ for $\min[v(\theta,\phi)] < v_0$. Note that there is no positive maximum error if $v(\theta,\phi) < v_0$, and no negative maximum error if $v(\theta,\phi) > v_0$ for all angles. The positive and negative maximum attenuation errors are also defined in a similar fashion. Such definitions

ensure that both "most positive" and "most negative" errors can be recorded.

Figures 3, 4 and 5 plot the positive and negative maximum phase velocity and attenuation errors with respect to $\sigma/\omega\epsilon$ at three cases of $\sigma^*/\omega\mu = 10^{-2}$, 10^0 and 10^2. N is 40 and Δt is the 3-D lossless Courant limit throughout the remaining sections. Although not shown, it is found that the phase velocity and attenuation errors recorded for $\sigma^*/\omega\mu = 0$ and $\sigma^*/\omega\mu = 10^{-2}$ are very similar. Hence it can be understood that the dispersion characteristics of doubly lossy media at low $\sigma^*/\omega\mu$ ($< 10^{-2}$) do not differ much from that of electrically lossy media. It should also be noted that not all regions have simultaneous positive and negative maximum errors. Some may have either only

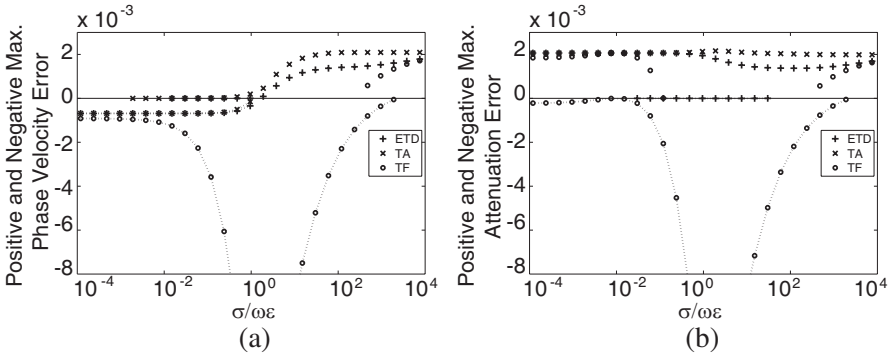

Figure 3. Positive and negative maximum (a) phase velocity and (b) attenuation errors with respect to $\sigma/\omega\epsilon$. $\sigma^*/\omega\mu = 10^{-2}$, $N = 40$. Dash lines represent negative maximum errors.

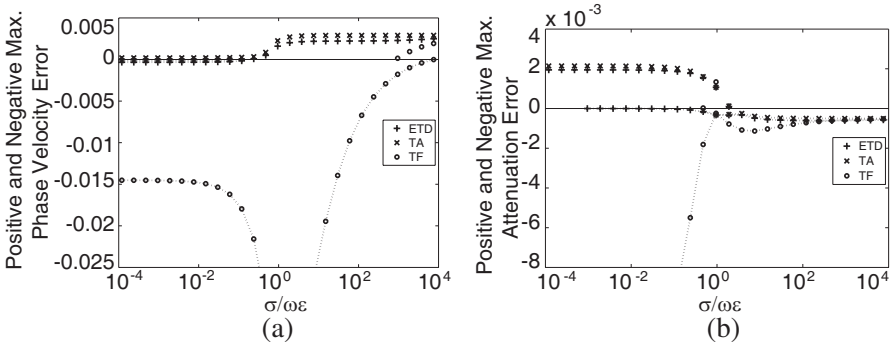

Figure 4. Same as Fig. 3, but for $\sigma^*/\omega\mu = 10^0$.

positive or negative errors across all propagation angles. Next, we observe that in all cases, TF (first-order) generally displays higher (absolute) maximum errors than ETD and TA (second-order), and its maximum errors are mostly negative. Further comparing ETD and TA, it can be seen again that ETD generally has lower maximum errors than TA.

We note that the dispersion errors of TF can sometimes be lower than ETD and TA for certain $\sigma/\omega\epsilon$ and $\sigma^*/\omega\mu$ during the transition between negative maximum and positive maximum errors (for instance, cf. Fig. 3). This effect is more pronounced in lower mesh density. To demonstrate this, Figs. 6 and 7 now plot the positive and negative maximum phase velocity and attenuation errors with respect to a range of frequencies at $N = 10$ and $N = 40$. Note that N is set with respect

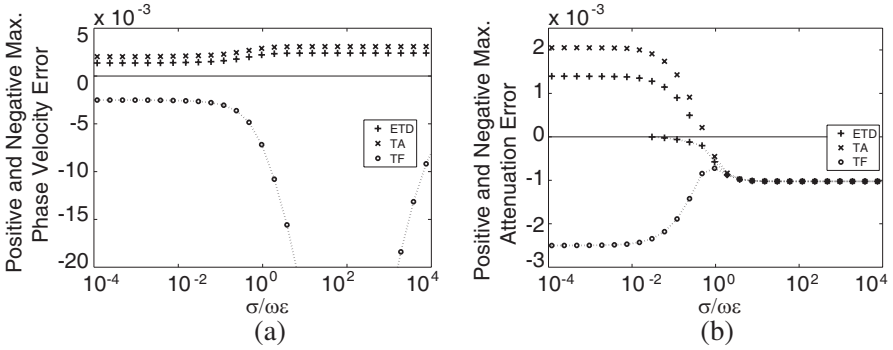

Figure 5. Same as Fig. 3, but for $\sigma^*/\omega\mu = 10^2$.

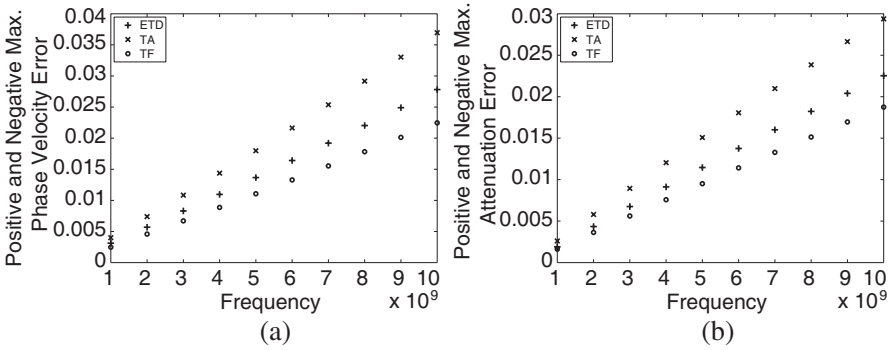

Figure 6. Positive and negative maximum (a) phase velocity and (b) attenuation errors with respect to frequency. No negative maximum errors here. $\sigma = 60\,\mathrm{S/m}$, $\sigma^* = 800\,\Omega/\mathrm{m}$, $N = 10$ at $f_{\max} = 10\,\mathrm{GHz}$.

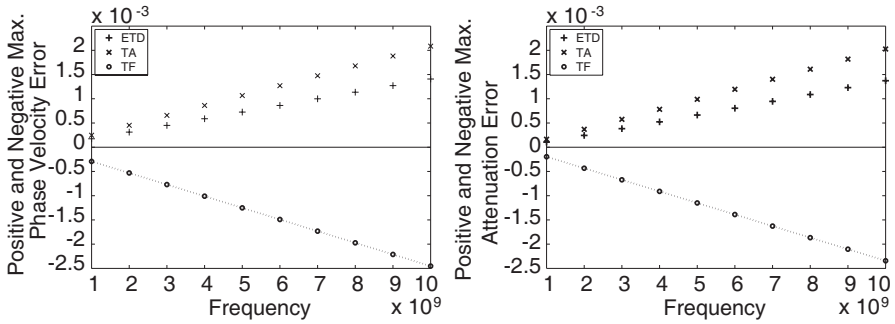

Figure 7. Same as Fig. 6, but for $N = 40$. Dash lines represent negative maximum errors.

to the highest frequency (10 GHz), and Δ shall remain invariant for other lower frequencies. σ and σ^* are arbitrarily set at 60 S/m and 800 Ω/m respectively. It can be seen that at $N = 10$ (low mesh density), the maximum phase velocity and attenuation errors exhibited by TF are lower than that of ETD and TA, and its maximum errors are in the same polarity as ETD and TA. At $N = 40$, the maximum errors of TF return to the highest among all. Such observations are somewhat similar to those found in [17], where higher order schemes do not necessarily yield lower dispersion errors at lower mesh density. Nevertheless, the dispersion errors of ETD are still lower than TA throughout.

Since the dispersion errors in 3-D differ at different angles, it is customary for us to define the phase velocity anisotropy error as $(\max[v(\theta,\phi)] - \min[v(\theta,\phi)])/\min[v(\theta,\phi)]$. The attenuation anisotropy error is also defined in the similar way. Note that the definition of anisotropy here is more appropriate compared to those in [9], where only diagonal and axial errors are taken in consideration. Figs. 8, 9 and 10 plot the phase velocity and attenuation anisotropy errors with respect to $\sigma/\omega\epsilon$ at $\sigma^*/\omega\mu = 10^{-2}$, 10^0 and 10^2. N is set at 40. ETD and TA have near similar anisotropy errors while TF has generally higher anisotropy errors than ETD and TA. However, it can also be seen that the anisotropy errors of TF can be lower than that of ETD and TA at certain higher range of $\mu''\epsilon''/\mu'\epsilon'$. Again, similar to previous phase velocity and attenuation errors, this can be mitigated by adopting higher mesh density.

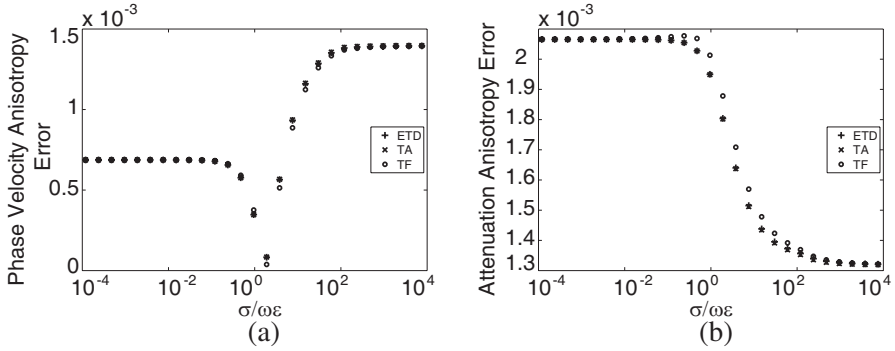

Figure 8. (a) Phase velocity and (b) attenuation anisotropy errors with respect to $\sigma/\omega\epsilon$. $\sigma^*/\omega\mu = 10^{-2}$, $N = 40$.

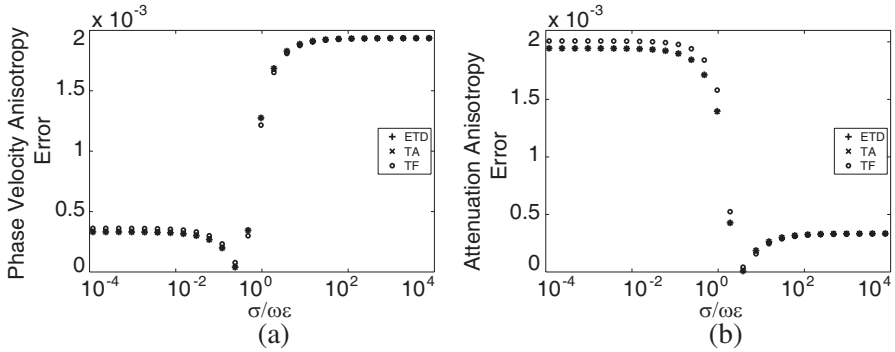

Figure 9. Same as Fig. 8, but for $\sigma^*/\omega\mu = 10^0$.

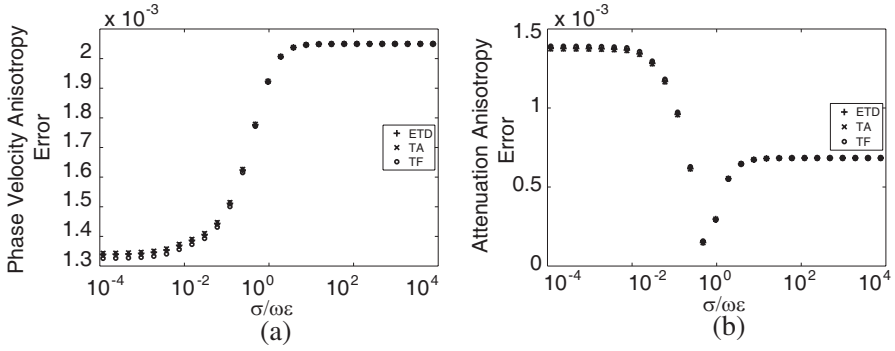

Figure 10. Same as Fig. 8, but for $\sigma^*/\omega\mu = 10^2$.

3.3. Numerical Simulation

In this subsection, further investigations with actual FDTD simulations in 1-D and 3-D are done. For 1-D, we use 100 cells of homogeneous doubly lossy medium with $\sigma = 10\,\mathrm{S/m}$ and $\sigma^* = 10^4\,\Omega/\mathrm{m}$. The values of σ and σ^* are chosen such that they are sufficiently large for clear demonstration of the doubly lossy effect, while ensuring measurable field values (not too severely attenuated). N is set at 10 ($\Delta z = 10\,\mu\mathrm{m}$) at the operating frequency of 100 GHz and $\Delta t = 0.811\,\mathrm{ps}$ is at the lossless 1-D Courant limit. A Gaussian pulse with significant frequency content of up to 100 GHz is launched as a hard source at the initial point. The analytical electric field in time domain at each cell position after arbitrary time step can be obtained by numerically integrating the frequency domain solution. This analytical electric field will serve as the reference solution to be compared with the simulated electric field. Fig. 11(a) plots the absolute electric field error normalized to the maximum amplitude of reference solution against cell position. The error exhibited by TF has fallen outside the range of the plot and is comparatively larger than ETD and TA. Between second-order ETD and TA, we can see that the error recorded by ETD is generally lower than that of TA.

For 3-D experiment, we consider a homogeneous doubly lossy medium filled cavity with $18 \times 18 \times 17$ dimension terminated by PEC walls. σ and σ^* are chosen as $0.1\,\mathrm{S/m}$ and $500\,\Omega/\mathrm{m}$ respectively. A z-directed point current source is located precisely at the centre $(10, 10, 9)$ of the cavity, driven by modulated Gaussian pulse with significant frequency content of up to 600 MHz. Again, $N = 10$ ($\Delta x = \Delta y = \Delta z = 36\,\mathrm{mm}$) at the operating frequency of 600 MHz is

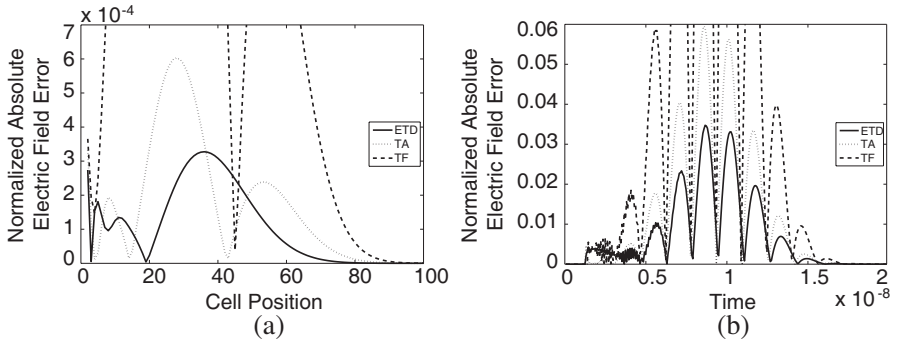

Figure 11. Normalized absolute electric field error with respect to (a) cell position for 1-D problem and (b) time for 3-D problem in a doubly lossy medium. $N = 10$.

chosen for the cell size, and $\Delta t = 69.267$ ps is at 3-D lossless Courant limit. The electric field is then recorded at position $(16, 16, 15)$ until the simulation is terminated after 20 ns. Using similar configuration, the cell size is reduced to 1/3 of the original problem and simulation is carried out using TA scheme with properly scaled dimension, cell size, and time step. This will serve as the reference solution for comparison. Fig. 11(b) plots the absolute electric field error normalized to the maximum amplitude of reference solution with respect to time. It can be seen that the error recorded by ETD is the lowest among all under such circumstances. Also, the overall errors recorded from 3-D experiment are larger than those recorded from 1-D. This may be due to the presence of anisotropy effects in 3-D. From all these simulations, we find that ETD is generally the better choice for modeling doubly lossy media compared to TA and TF.

4. CONCLUSION

This paper has presented the 3-D dispersion analysis of FDTD schemes for doubly lossy media, where both electric and magnetic conductivities are nonzero. It has been shown that, unlike in electrically lossy media, the attenuation constant in doubly lossy media can be larger than its phase constant. This further calls for careful choice of cell size such that both wavelength and skin depth of the doubly lossy media are properly resolved. From the dispersion analysis, TF generally displays higher phase velocity and attenuation errors due to its first-order temporal accuracy nature compared to second-order ETD and TA. Although both have second-order temporal accuracy, ETD has generally lower phase velocity and attenuation errors than TA. This may be attributed to its closer resemblance to the solution of first-order differential equation. Numerical FDTD simulations in 1-D and 3-D further confirm these findings. Owing to its higher accuracy, ETD should be better than TA for FDTD simulation of doubly lossy or electrically lossy media.

REFERENCES

1. Taflove, A. and S. C. Hagness, *Computational Electrodynamics: The Finite-difference Time-domain Method*, Artech House, Boston, M. A., 2005.
2. Luebbers, R., K. Kumagai, S. Adachi, and T. Uno, "FDTD calculation of transient pulse propagation through a nonlinear magnetic sheet," *IEEE Trans. Electromagn. Compat.*, Vol. 35, No. 1, 90–94, Feb. 1993.

3. Taflove, A. and M. E. Brodwin, "Numerical solution of steady-state electromagnetic scattering problems using the time-dependent Maxwell's equations," *IEEE Trans. Microw. Theory Tech.*, Vol. 23, No. 8, 623–630, Aug. 1975.
4. Holland, R., L. Simpson, and K. S. Kunz, "Finite-difference analysis of EMP coupling to lossy dielectric structures," *IEEE Trans. Electromagn. Compat.*, Vol. 22, No. 3, 203–209, Aug. 1980.
5. Petropoulos, P. G., "Analysis of exponential time-differencing for FDTD in lossy dielectrics," *IEEE Trans. Antennas Propagat.*, Vol. 45, No. 6, 1054–1057, Jun. 1997.
6. Pereda, J. A., O. Garcia, A. Vegas, and A. Prieto, "Numerical dispersion and stability analysis of the FDTD technique in lossy dielectrics," *IEEE Microw. Guided Wave Lett.*, Vol. 8, No. 7, 245–247, Jul. 1998.
7. Velarde, L. F., J. A. Pereda, A. Vegas, and O. Gonzalez, "A weighted-average scheme for accurate FDTD modeling of electromagnetic wave propagation in conductive media," *IEEE Antennas Propagat. Lett.*, Vol. 3, No. 7, 302–305, 2004.
8. Schuster, C., A. Christ, and W. Fichtner, "Review of FDTD time-stepping schemes for efficient simulation of electric conductive media," *Microwave Opt. Technol. Lett.*, Vol. 25, No. 1, 16–21, Apr. 2000.
9. Sun, G. and C. W. Trueman, "Numerical dispersion and numerical loss in explicit finite-difference time-domain methods in lossy media," *IEEE Trans. Antennas Propagat.*, Vol. 53, No. 11, 3684–3690, Nov. 2005.
10. Berenger, J.-P., "A perfectly matched layer for the absorption of electromagnetic waves," *Journal of Computational Physics*, Vol. 114, No. 2, 185–200, 1994.
11. Yurshevich, V. and S. Lomov, "Measurement of magnetic spectra of ferrites: Introducing a correction for ferrites dielectric parameters," *Measurement Science Review*, Vol. 3, No. 3, 41–44, 2003.
12. Singh, A. K., A. Verma, O. P. Thakur, C. Prakash, T. C. Goel, and R. G. Mendiratta, "Electrical and magnetic properties of Mn-Ni-Zn ferrites processed by citrate precursor method," *Materials Lett.*, Vol. 57, Nos. 5–6, 1040–1044, Jan. 2003.
13. Hyde IV, M. W. and M. J. Havrilla, "A nondestructive technique for determining complex permittivity and permeability of magnetic sheet materials using two flanged rectangular waveguides," *Progress In Electromagnetics Research*, PIER 79, 367–386, 2008.

14. Lee, J. P. Y. and K. G. Balmain, "Wire antennas coated with magnetically and electrically lossy material," *Radio Science*, Vol. 14, No. 3, 437–445, May 1979.
15. Du, J.-H., C. Sun, S. Bai, G. Su, Z. Ying, and H.-M. Cheng, "Microwave electromagnetic characteristics of a microcoiled carbon fibers/paraffin wax composite in Ku band," *Journal of Materials Research*, Vol. 17, No. 5, 1232–1236, May 2002.
16. Ulaby, F., *Fundamentals of Applied Electromagnetics*, 5th Edition, Prentice Hall, 2007.
17. Tan, E. L. and D. Y. Heh, "ADI-FDTD method with fourth order accuracy in time," *IEEE Microw. Wireless Compon. Lett.*, Vol. 18, No. 5, 296–298, May 2008.